

# Maximum power point tracking using adaptive fuzzy logic control for grid-connected photovoltaic system

Nopporn Patcharaprakiti<sup>a,1</sup>, Suttichai Premrudeepreechacharn<sup>b,\*</sup>,  
Yosanai Sriuthaisiriwong<sup>b,2</sup>

<sup>a</sup>*Department of Electrical Engineering, Rajamagala Institute of Technology, Chiang Rai 57120, Thailand*

<sup>b</sup>*Department of Electrical Engineering, Chiang Mai University, Chiang Mai 50200, Thailand*

---

## Abstract

This paper proposes a method of maximum power point tracking using adaptive fuzzy logic control for grid-connected photovoltaic systems. The system is composed of a boost converter and a single-phase inverter connected to a utility grid. The maximum power point tracking control is based on adaptive fuzzy logic to control a switch of a boost converter. Adaptive fuzzy logic controllers provide attractive features such as fast response, good performance. In addition, adaptive fuzzy logic controllers can also change the fuzzy parameter for improving the control system. The single phase inverter uses predictive current control which provides current with sinusoidal waveform. Therefore, the system is able to deliver energy with low harmonics and high power factor. Both conventional fuzzy logic controller and adaptive fuzzy logic controller are simulated and implemented to evaluate performance. Simulation and experimental results are provided for both controllers under the same atmospheric condition. From the simulation and experimental results, the adaptive fuzzy logic controller can deliver more power than the conventional fuzzy logic controller.

© 2005 Published by Elsevier Ltd.

*Keywords:* Adaptive fuzzy logic control; Maximum power point tracking; Photovoltaic system

---

## 1. Introduction

Photovoltaic (PV) energy has increased interest in electrical power applications. It is crucial to operate the PV energy conversion systems near the maximum power point to increase the efficiency of the PV system. However, the nonlinear nature of PV system is apparent from Fig. 1, i.e. the current and power of the PV array depends on the array terminal operating voltage. In addition, the maximum power operating point varies with insolation level and temperature. Therefore, the tracking control of the maximum power point is a complicated problem. To overcome these problems, many tracking control strategies have been proposed such as perturb and observe [1,2], incremental conductance [3], parasitic capacitance [4], constant voltage [5], neural network [6–10] and fuzzy logic controller (FLC) [11–14]. These strategies have some disadvantages such as high cost, difficulty, complexity and instability.

The general requirements for maximum power point tracking (MPPT) are simplicity and low cost, quick tracking under changing conditions, and small output power fluctuation. A more efficient method to solve this problem becomes crucially important. Hence, this paper proposes a method to track maximum power point using adaptive fuzzy logic controller (AFLC). FLC is appropriate for non-linear control. In addition, FLC does not use complex mathematic. Behaviors of FLC depend on shape of membership functions and rule base. There is no formal method to determine accurately the parameters of the controller. However, choosing fuzzy parameters to yield optimum operating point and a good control system depends on the experience of designer. FLC with fixed parameters are inadequate in application where the operating conditions change in a wide range

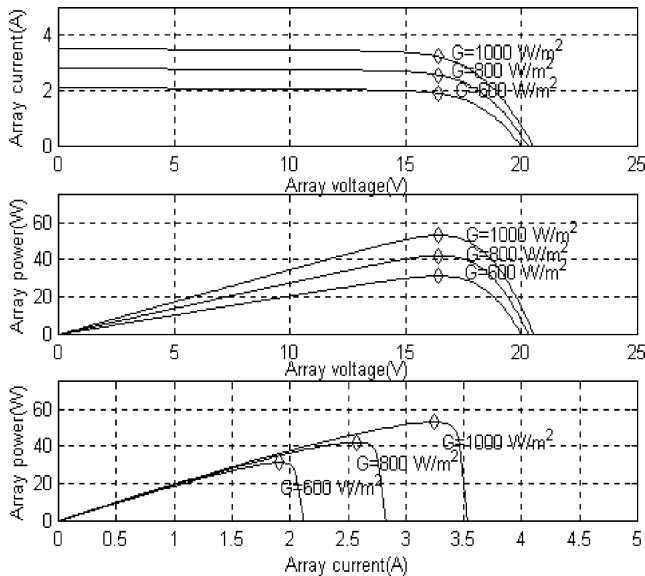


Fig. 1. PV array characteristics.

and the available expert knowledge is not reliable. AFLC can solve this problem because it can re-adjust the fuzzy parameters to obtain optimum performance.

## 2. Grid-connected photovoltaic system

In order to investigate the feasibility of MPPT using AFLC, a photovoltaic power system with a boost converter and a single phase inverter is constructed as shown in Fig. 2.

### 2.1. Boost converter

A boost converter can be used to increase voltage magnitude for an inverter circuit and to control MPPT. AFLC and pulse width modulation (PWM) method is used to generate a pulse for drive controllable switch (SB). The output voltage of the boost converter can be calculated from

$$\frac{V_o}{V_{in}} = \frac{1}{1 - \text{Duty}} \tag{1}$$

where  $V_{in}$  is the input voltage (output voltage of PV array),  $V_o$  is the output voltage and Duty the duty ratio of controllable switch.

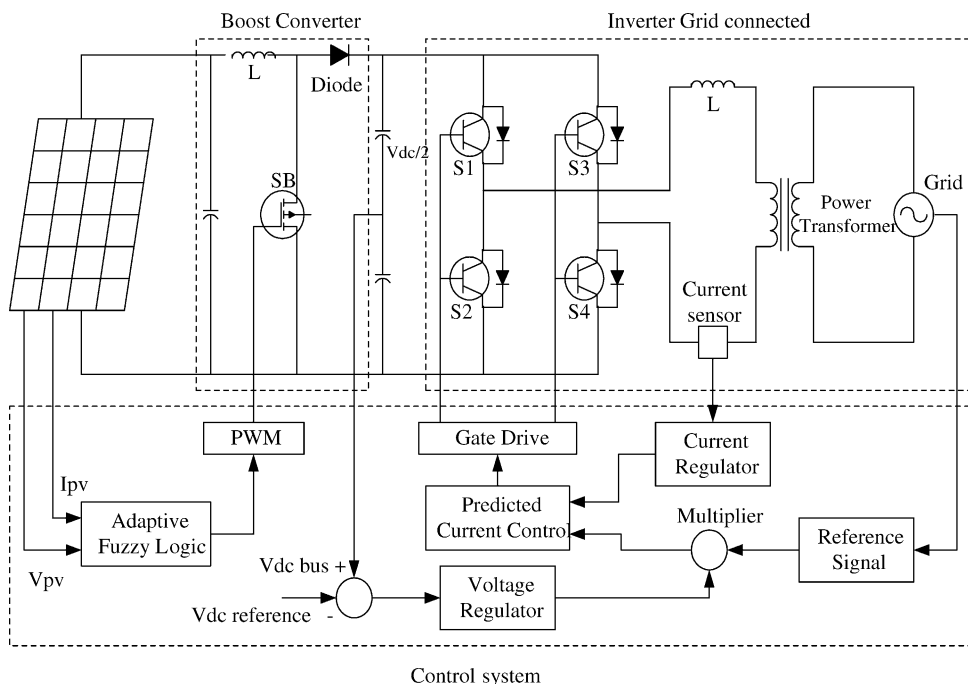


Fig. 2. Grid-connected photovoltaic system.

## 2.2. Single phase inverter

The inverter circuit converts direct current to alternating current by using predictive current control. Predictive current control provides current with sinusoidal waveform. Therefore, the system is able to deliver energy with low harmonics and high power factor. The controller for single phase inverter is described in Section 4. The inverter circuit is composed of a DC source from a boost chopper circuit, four controllable switches (S1–S4), an inductance, and a transformer.

## 3. Adaptive fuzzy logic controller

Traditional FLC requires the expert knowledge of the process operation for the FLC parameter setting, and the controller can be only as good as the expertise involved in the design. FLC with a fixed parameter is inadequate in applications when the operating conditions change in a wide range and the available expert knowledge is not reliable. To make the controller less dependent on the expert knowledge, AFLC could be introduced. However, the computation cost is much higher than conventional FLC. AFLC as shown in Fig. 3 is composed of two parts: fuzzy knowledge base controller and a learning mechanism.

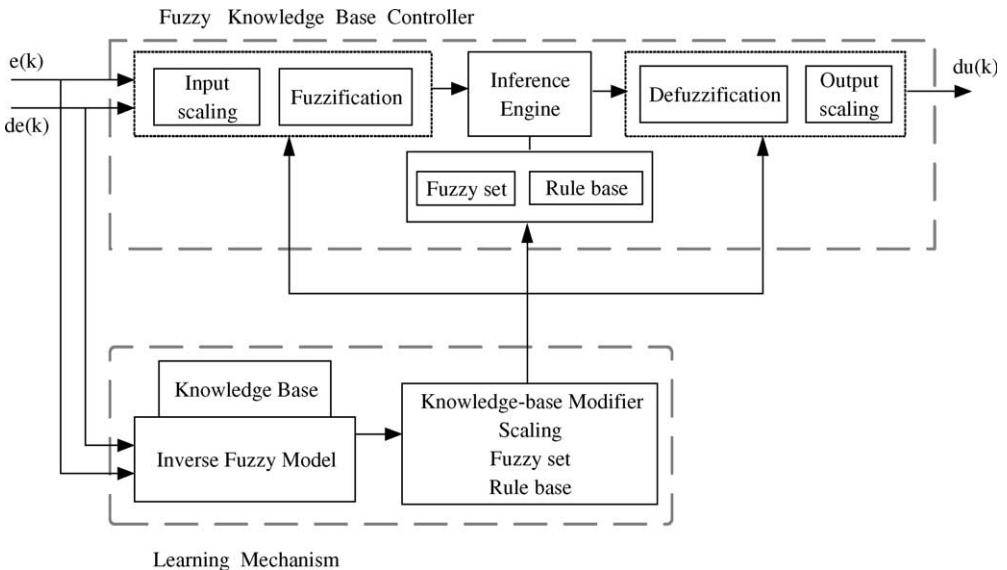


Fig. 3. Structure of adaptive fuzzy logic controller.

### 3.1. Fuzzy knowledge-base controller

The fuzzy knowledge-base controller is one part of FLC which is composed of three main parts: fuzzification, inference engine and defuzzification.

#### 3.1.1. Fuzzification

Membership function values are assigned to the linguistic variables, using seven fuzzy subsets: NB (negative big), NM (negative medium), NS (negative small), ZE (zero), PS (positive small), PM (positive medium), and PB (positive big). The partition of fuzzy subsets and the shape of membership function, which can adapt shape up to appropriate system, are shown in Fig. 4. The value of input error ( $e$ ) and change of error ( $de$ ) are normalized by an input scaling factor. In this system the input scaling factor has been designed such that input values are between  $-1$  and  $1$ .

The triangular shape of the membership function of this arrangement presumes that for any particular input there is only one dominant fuzzy subset. The input error ( $e$ ) for the fuzzy logic controller can be calculated from the maximum power point as follows

$$E(k) = \frac{\Delta I}{\Delta V} + \frac{I}{V} = \frac{\Delta P}{\Delta V} = \frac{\Delta P}{\Delta I} \quad (2)$$

where  $I$  is the output current from PV array,  $\Delta I$  is the change of output current,  $I(k) - I(k - 1)$ ,  $V$  is output voltage from PV array,  $\Delta V$  is change of output voltage,  $V(k) - V(k - 1)$ .

#### 3.1.2. Inference method

The composition operation is the method by which a control output is generated. Several composition methods such as Max-Min and Max-Dot have been proposed in the literature. The commonly used method, Max-Min, is used in this paper. The output membership function of each rule is given by the Min (minimum) operator and Max (maximum) operator. Table 1 shows rule base of the FLC.

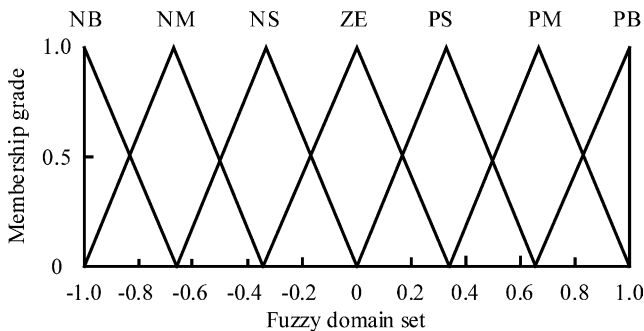


Fig. 4. Fuzzy logic control membership function for input and output.

Table 1  
Rule base of fuzzy logic controller

Error ( <i>e</i> )	Change of error ( <i>de</i> )						
	NB	NM	NS	ZE	PS	PM	PB
NB	NB	NB	NB	NB	NM	NS	ZE
NM	NB	NB	NB	NM	NS	ZE	PS
NS	NB	NB	NM	NS	ZE	PS	PM
ZE	NB	NM	NS	ZE	PS	PM	PB
PS	NM	NS	ZE	PS	PM	PB	PB
PM	NS	ZE	PS	PM	PB	PB	PB
PB	ZE	PS	PM	PB	PB	PB	PB

### 3.1.3. Defuzzification

As a plant usually requires a nonfuzzy value of control, a defuzzification stage is needed. Defuzzification for this system is the height method which is both simple and fast, and is in a system of *m* rules given by

$$du = \left( \frac{\sum_{k=1}^m c(k) * w_k}{\sum_{k=1}^m w_k} \right) \quad (3)$$

where *du* is the change of control output, *c(k)* is the peak value of each output and *w<sub>k</sub>* is height of rule *k*.

The output of FLC is used to modify control output. Then, control output is compared with the sawtooth waveform to generate a pulse for controllable switch (SB) of the boost converter.

## 3.2. Learning mechanism

The purpose of the learning mechanism is to learn the environmental parameters and to modify the FLC accordingly so that the response of the overall system is close to the optimum operation point. The learning mechanism is composed of an inverse fuzzy model and a knowledge base modifier.

### 3.2.1. Inverse fuzzy model

The error (*e*) or the change of error (*de*) of the system and the knowledge base modifier are used to modify the fuzzy parameter to optimize the system operation. The fuzzy parameter can be adapted by using the following condition:

If  $\text{error} < \varepsilon$  (limit value) then knowledge base modifier will be chosen.

### 3.2.2. Knowledge base modifier

In this part fuzzy parameter will be modified as follows [15].

**3.2.2.1. Scaling factor.** Simple schemes for altering the scaling factor to meet various performance criteria can be devised. When a scaling factor of a fuzzy variable is changed, the definition of each membership function will be changed by the same ratio. Hence,

Table 2  
Learning mechanism of adaptive fuzzy logic control

Invert fuzzy model		Knowledge base modifier	
Error ( $e(k)$ )	Change of error ( $de(k)$ )	Peak of membership	Scaling factor
$-\varepsilon < e(k) < \varepsilon$	$-\varepsilon < de(k) < \varepsilon$	$c(k)$	$e(k) = e(k) * \delta_3$
$e(k) > \varepsilon$	$-\varepsilon < de(k) < \varepsilon$	$c(k) + \delta_2$	Unchanged
$e(k) > \varepsilon$	$de(k) > \varepsilon$	$c(k) + \delta_1$	Unchanged
$e(k) > \varepsilon$	$de(k) < -\varepsilon$	$c(k)$	$E(k) = e(k) * \delta_3$
$e(k) < -\varepsilon$	$-\varepsilon < de(k) < \varepsilon$	$c(k) - \delta_2$	Unchanged
$e(k) < -\varepsilon$	$de(k) > \varepsilon$	$c(k)$	$E(k) = e(k) * \delta_3$
$e(k) < -\varepsilon$	$de(k) < -\varepsilon$	$c(k) - \delta_1$	Unchanged

$\varepsilon$  is the minimum of error,  $c(k)$  is the peak of triangle membership  $k$ .

changing of any scaling factor can change the meaning of one part of any rule. The relation between the error, change of error, and output of FLC is similar to relation of conventional proportional and integral controller.

**3.2.2.2. Fuzzy set membership function.** Tuning peak values, such as error in Fig. 4, can improve both responsiveness and stability. A large error, NM and PM, can improve responsiveness. While a small error, NS and PS, can improve stability. Changing of width of membership affects the interpolation between two peak values. The modification can be performed by shifting the membership functions of both input and output.

**3.2.2.3. Tuning rule base.** Modifying rule base can affect the control system such as overshoot, setting time, stability, and responsiveness. When the fuzzy set membership function is modified, it may affect some rule bases. However, when a rule is changed, only this rule is involved. The modification is performed by adjusting the rule such that the rule firing trajectory always moves toward the stable point.

The learning mechanism of AFLC is shown in Table 2. The input for the invert fuzzy model is error and change of error. While the output of the knowledge base modifier are the change of peak of membership and scaling factor. In this paper,  $\varepsilon = 0.1$ ,  $\delta_1 = 0.1$ ,  $\delta_2 = 0.2$ , and  $\delta_3 = 0.1$  are used to modify the peak of membership and scaling factor for AFLC.

#### 4. Predicted current control

From the predicted current control described in [16], line current can be defined as

$$\Delta I = I(t_n + T_s) - I(t_n) = [V_s(t_n) - V_{inv}(t_n)]T_s/L \quad (4)$$

where  $I$  is the inverter line current,  $V_s$  is utility voltage and  $V_{inv}$  the output voltage of inverter.

The output voltage of inverter ( $V_{inv}$ ) can be calculated from (5) as follows:

$$V_{inv(t_n)} = V_s(t_n) - (L/T_s)[I(t_n + T_s) - I(t_n)] \quad (5)$$

The current of a single phase inverter can be controlled by controlling switches S1–S4. The switches S1 and S2 are used to shape the waveform to follow the reference current. While the switches S3 and S4 are used to correct the polarity of the waveform. Hence, the  $V_{inv}$  can be described as follows

$$V_{inv} = d_k V_{dc} \quad (6)$$

where  $d_k$  is the duty ratio for switch S1 and S2 over one switching period and  $V_{dc}$  is the DC bus voltage from boost converter.

The change in line current over one period can be defined as:

$$\Delta I = I(t_n + T_s) - I(t_n) = I(t_n) - I(t_n - t_s) \quad (7)$$

From (5)–(7), the duty ratio for single phase inverter can be defined as a function of source voltage ( $V_s$ ) and the change in line current ( $\Delta I$ ) as follows:

$$d_k = f(V_s, \Delta I) = \frac{1}{V_{dc}} \left( V_s - \frac{L\Delta I}{T_s} \right) \quad (8)$$

We will use (8) to control the duty ratio of switch S1 and S2 for the single phase inverter.

## 5. Simulation results

This section discusses the simulations of a grid-connected photovoltaic system shown in Fig. 2. The MPPT was controlled by using AFLC. While inverter circuit uses predicted current control in order to have the output current as a sinusoidal waveform.

This system was simulated to learn the operation of the PV-grid connected system by using MATLAB. The system components of Fig. 2 which are used in the simulation are described in Table 3. The PV array was simulated using the model described in [2]. In this simulation, insolation level ( $G$ ) is changed from 800 to 600 W/m<sup>2</sup> at 0.008 s and then changed from 600 to 1000 W/m<sup>2</sup> at 0.015 s. The conventional FLC uses a rule base as

Table 3

The components used in simulation the system shown in Fig. 2

PV array	Power rating	55 W
	Open-circuit voltage ( $V_{oc}$ )	21.2 V
	Short-circuit current ( $I_{sc}$ )	3.54 A
	Series resistance ( $R_s$ )	0.39 $\Omega$
	Shunt resistance ( $R_{sh}$ )	176 $\Omega$
Boost converter	Inductor ( $L_{con}$ )	1 mH
	Capacitor ( $C_{con}$ )	4700 $\mu$ F
Single phase inverter	Inductor ( $L_{inv}$ )	3 mH
	AC source ( $V_{AC}$ )	220 V
	Line frequency	50 Hz

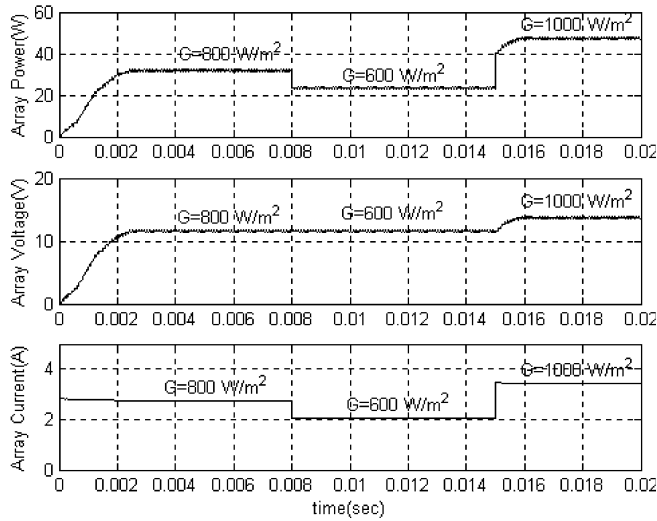


Fig. 5. Simulation results of conventional fuzzy logic controller.

shown in Table 1 and the membership function as shown in Fig. 4. The tracking of maximum power of a PV system by using conventional FLC is shown in Fig. 5. The PV characteristic using MPPT control with conventional FLC relative to the theoretical means of MPPT is illustrated in Fig. 6. It is found that the operating point of a PV system does not operate at the maximum power point.

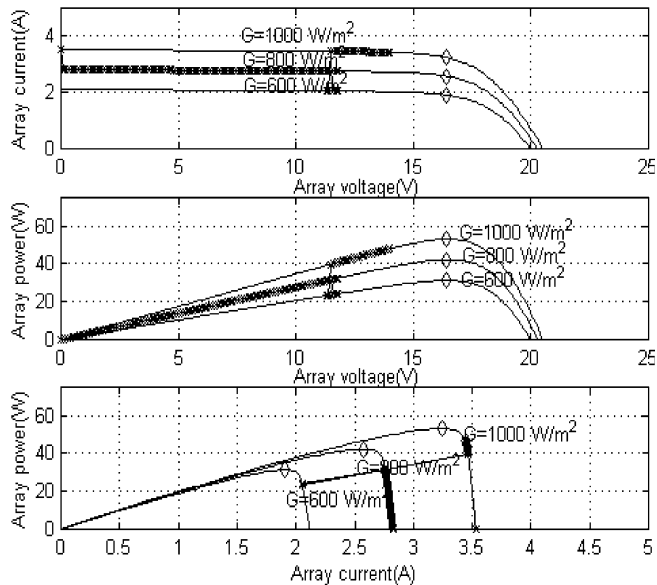


Fig. 6. Simulation results of conventional fuzzy logic controller versus theoretical PV array characteristic.

Table 4  
Rule base of fuzzy logic after change the rule base

Error ( $e$ )	Change of error ( $de$ )						
	NB	NM	NS	ZE	PS	PM	PB
NB	NB	NB	NM	ZE	ZE	ZE	ZE
NM	NB	NM	NM	ZE	NM	PS	PS
NS	NB	NB	NB	NB	PM	PS	PM
ZE	NB	NB	NS	ZE	PS	PM	PB
PS	NM	NS	ZE	PS	PM	PB	PB
PM	NS	PB	PB	PB	PB	PB	PB
PB	PB	PB	PB	PB	PB	PB	PB

From the learning mechanism as described in Section 3, the new rule base for the controller is shown in Table 4 and fuzzy membership function of error ( $e$ ) after adaptation is shown in Fig. 7. The insolation level ( $G$ ) is changed from 800 to 600 W/m<sup>2</sup> at 0.008 s and then changed from 600 to 1000 W/m<sup>2</sup> at 0.015 s. The AFLC can improve the MPPT controller as seen from Figs. 8 and 9. From simulation, Fig. 8 shows the tracking of maximum power of PV system after parameter adaptation. Fig. 9 shows the PV characteristics using MPPT control with AFLC relative to the theoretical means of MPPT. When comparing the result in Fig. 6 with those of Fig. 9, it is clear that the operating point of this system operates closer to a maximum power point than conventional FLC before parameter adaptation. Thus, the tracking operating point of the MPPT controller is improved by using AFLC. Fig. 10 shows output of converter voltage and output of inverter current. Therefore, the system is able to deliver energy to a utility with low harmonics and a high power factor.

## 6. Experimental results

This section discusses the operation of the system shown in Fig. 2. The system was built and experimentally evaluated to learn more about the operation of MPPT using AFLC.

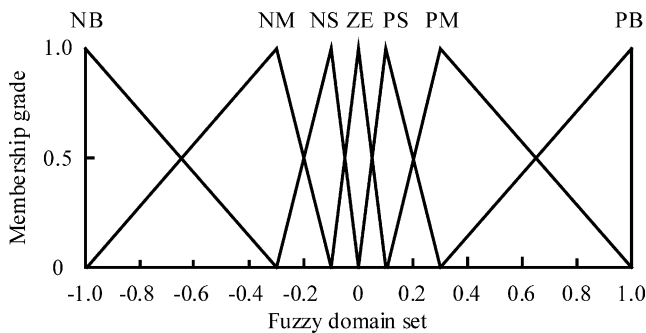


Fig. 7. Fuzzy logic control membership function of error ( $e$ ) after adjusted the shape of membership function.

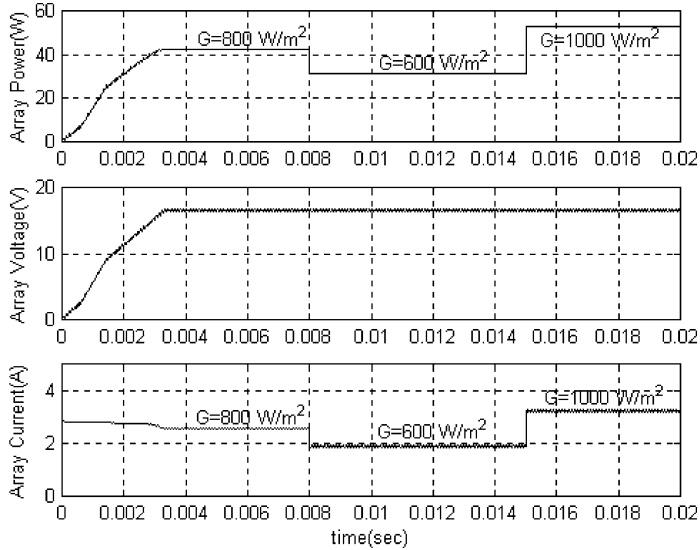


Fig. 8. Simulation results of adaptive fuzzy logic controller.

The system components, Fig. 2, used in the experiment are described in Table 5. For comparison purposes, the AFLC and conventional FLC have been implemented to evaluate the performance using the same grid-connected system.

The PV array is made up of two PV panels connected in series. The DC/DC converter consists of a single stage boost converter that is responsible for the displacement the PV

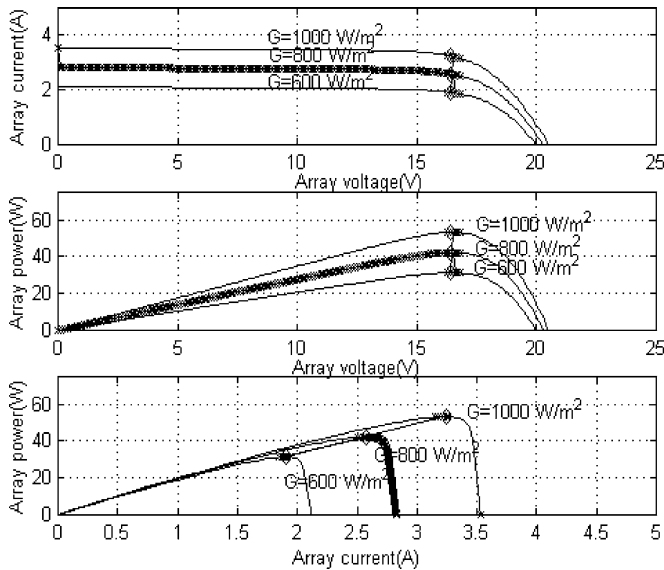


Fig. 9. Simulation results of adaptive fuzzy logic controller versus theoretical PV array characteristic.

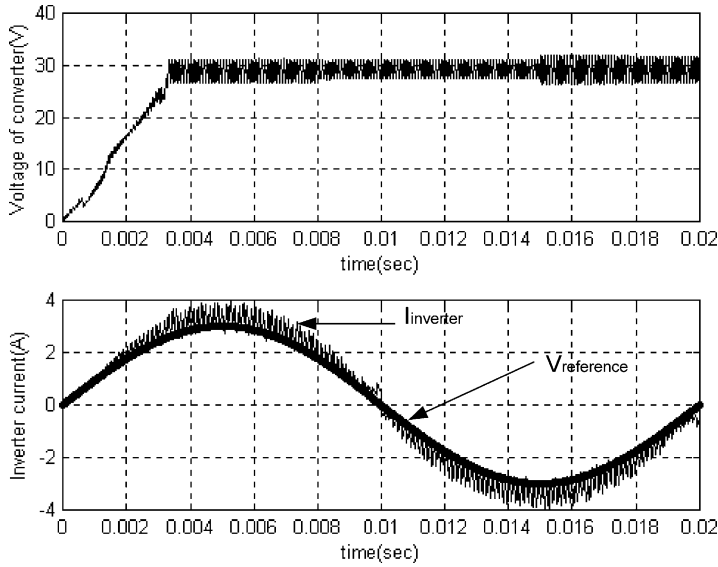


Fig. 10. Voltage output of converter and inverter current.

system operating point to the maximum power operation point. The PV array surface temperature is measured using a thermocouple. Also, the insolation level is measured using a pyranometer sensor.

Both the AFLC and conventional FLC are implemented using a microcomputer associated to a data acquisition hardware containing A/D and D/A converters. The A/D converter is used to link the analogue signal from the PV array data to the digital controller, while the D/A converter links the controller output to the boost converter. The DC/AC converter uses a single phase inverter with predictive current control. The DC/AC converter is responsible for the interconnection between the PV system and the grid.

Table 5  
The components used in implementing the system shown in Fig. 2

PV array	PV power	55 W
	PV model	BP1255
Boost converter	Switch (SB)	IRFP460
	Diode	MUR1569
	Inductor ( $L_{con}$ )	1 mH
	Capacitor ( $C_{con}$ )	4700 $\mu$ F
Single phase inverter	Switches (S1–S4)	HGTG20N60B3
	Inductor ( $L_{inv}$ )	3 mH
	Transformer ratio	7:220
	AC source ( $V_{AC}$ )	220 V
	Line frequency	50 Hz

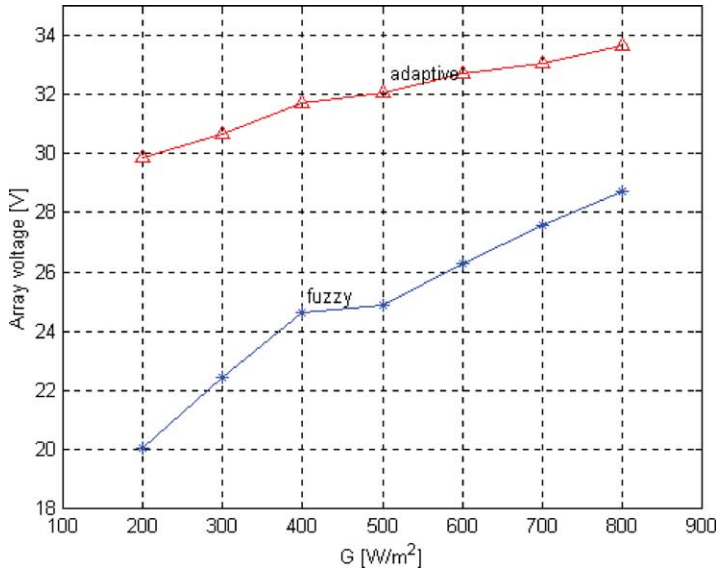


Fig. 11. Relation between insolation level and PV array voltage for both controllers.

Figs. 11–16 compare the performance of the system using the AFLC and conventional FLC for various insolation levels. The experimental results are collected from both controllers under the same atmospheric condition. Figs. 11 and 12 show the relationship between the insolation level and PV array voltage and PV array current, respectively. It can be seen that the AFLC provides more PV array voltage

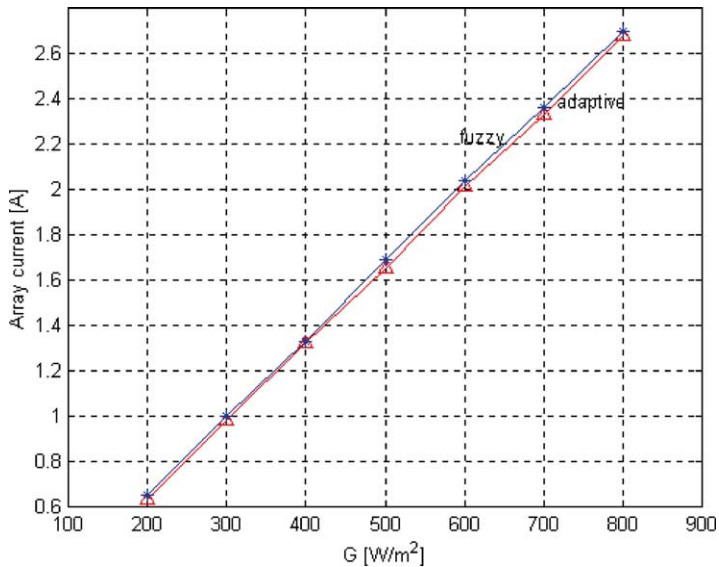


Fig. 12. Relation between insolation level and PV array current for both controllers.

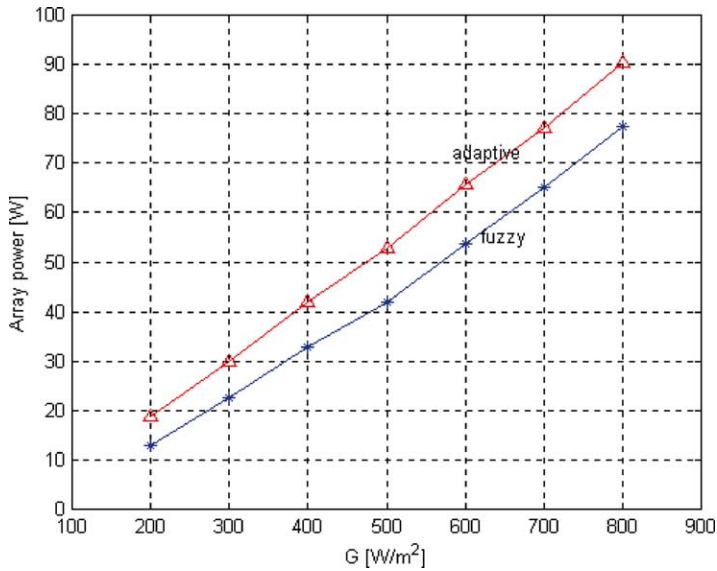


Fig. 13. Relation between insolation level and PV array power for both controllers.

and current than the conventional FLC. Thus, the AFLC is able to deliver more PV array power than the conventional FLC as shown in Fig. 13.

The experimental data are recorded for different atmospheric conditions and the graphs are plotted for two cases: AFLC and conventional FLC. Figs. 14–16 demonstrate

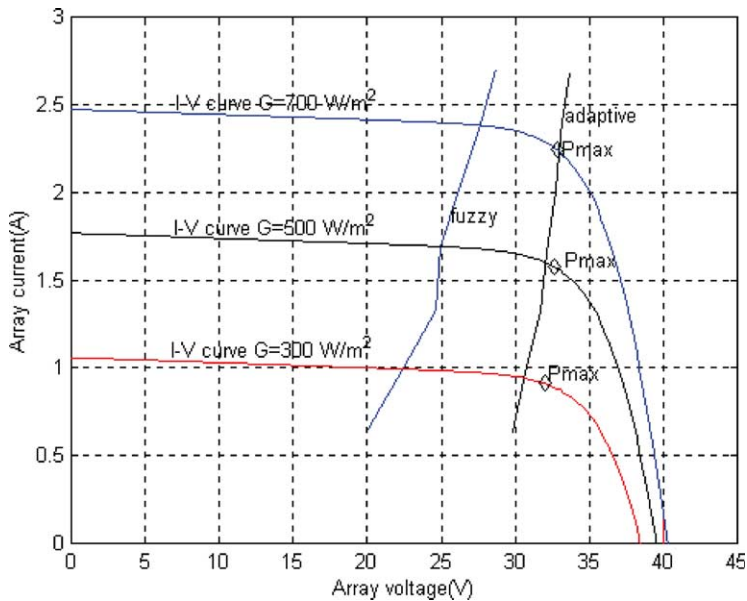


Fig. 14. Relation between PV array voltage and current for both controllers.

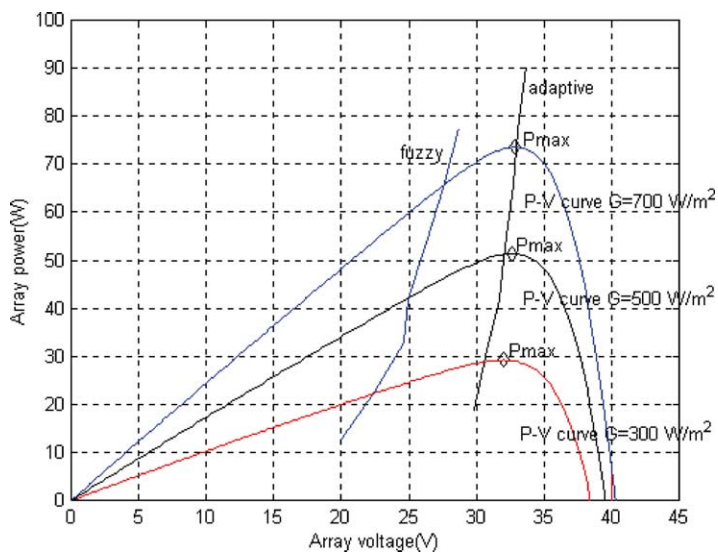


Fig. 15. Relation between PV array voltage and power for both controllers.

the MPPT for both controllers. The PV array characteristic curves in these figures are calculated from PV array parameters as described in the Section 5. As seen from these figures, the AFLC provides the power output from the PV array closer to the maximum power point when the insolation level gets higher.

The efficiency of the system is shown in Fig. 17 and depends on the insolation level. When the insolation is high, the system can delivery more power to the grid. The reference

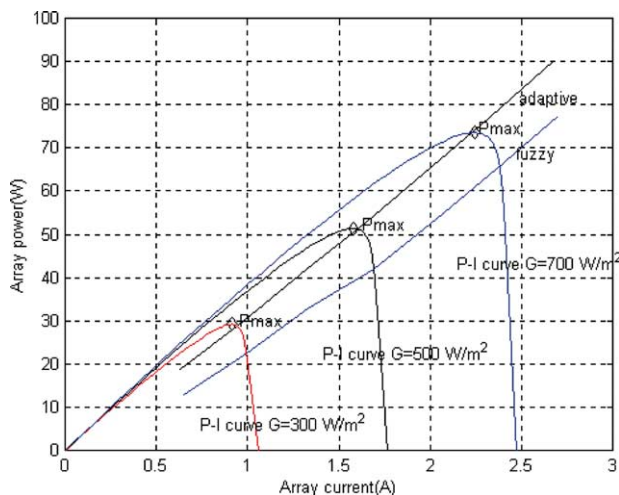


Fig. 16. Relation between PV array current and power for both controllers.

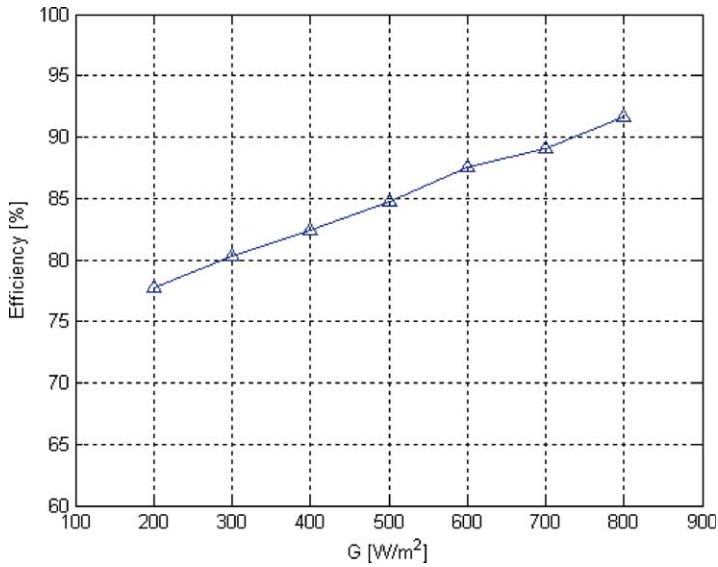


Fig. 17. Efficiency of system.

voltage and inverter current are shown in Fig. 18. As seen from this figure, the inverter current follows the reference voltage which is grid voltage. Therefore, the system provides the power to utility with unity power factor. The total harmonic distortion (THD) of inverter current is shown in Fig. 19. From Fig. 19, the THD is decreasing because

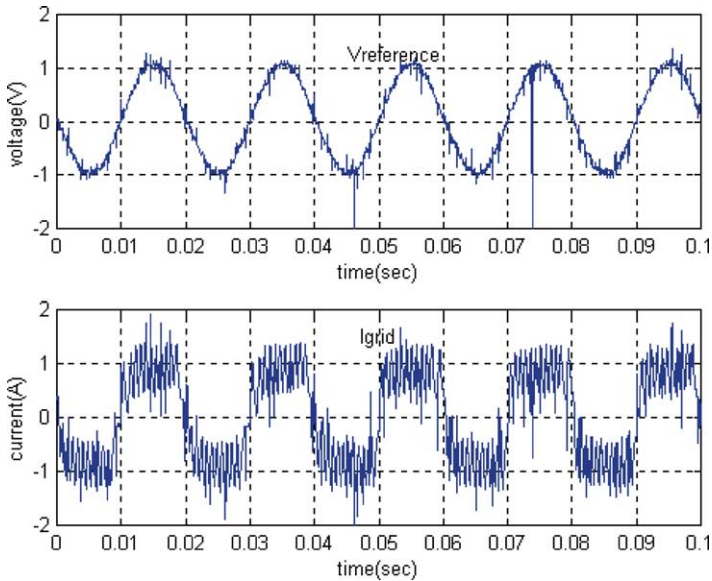


Fig. 18. Reference voltage and current of inverter.

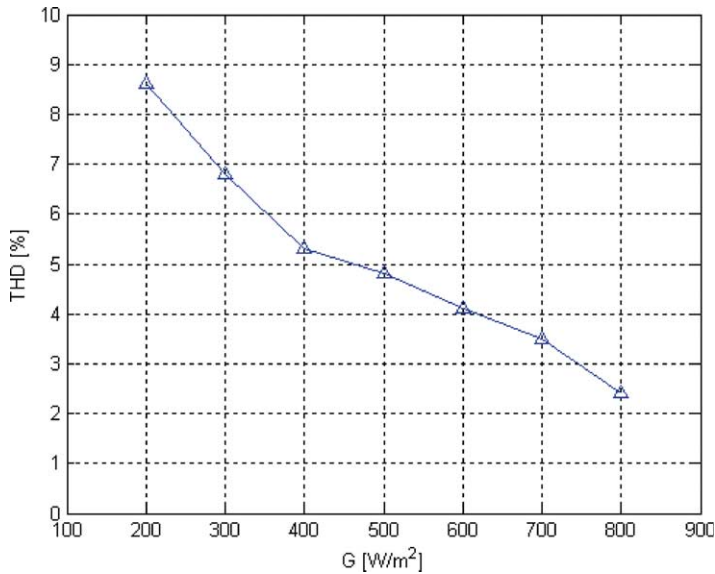


Fig. 19. Total harmonic distortion of current.

the fundamental of inverter current is increasing while the higher frequency components are almost the same.

## 7. Conclusions

This paper has presented the AFLC for controlling MPPT of a grid-connected photovoltaic system. The proposed algorithm in AFLC was simulated. The simulation results show that this system is able to adapt the fuzzy parameters for fast response, good transient performance, insensitive to variations in external disturbances. In addition, the results of simulation and experiment have shown that MPPT controllers by using AFLC have provided more power than conventional. This system can provide energy to a utility with low harmonics and high power factor.

## References

- [1] Hua C, Shen C. Comparative study of peak power tracking techniques for solar storage system. IEEE Appl Power Electron Conf Exposition Proc 1998;2:679–83.
- [2] Hussein KH, Muta I, Hoshino T, Osakada M. Maximum photovoltaic power tracking: an algorithm for rapidly changing atmospheric conditions. IEEE Proc Generation Transmission Distribution 1995;142(1): 59–64.
- [3] Brambilla A. New approach to photovoltaic arrays maximum power point tracking. Proc 30th IEEE Power Electron Specialists Conf 1998;2:632–7.

- [4] Hohm DP, Ropp ME. Comparative study of maximum power point tracking algorithm using an experimental, programmable, maximum power point tracking test bed. Proc 28th IEEE Photovoltaic Specialist Conf 2000;28:1699–702.
- [5] Swiegers W, Enslin J. An integrated maximum power point tracker for photovoltaic panels. Proc IEEE Int Symp Ind Electron 1998;1:40–4.
- [6] Hiyama T, Kitabayashi K. Neural network based estimation of maximum power generation from PV module using environment information. IEEE Trans Energy Conversion 1997;12(3):241–7.
- [7] Hiyama T, Kouzuma S, Imakubo T, Ortmeyer TH. Evaluation of neural network based real time maximum power tracking controller for PV system. IEEE Trans Energy Conversion 1995;10(3):543–8.
- [8] Hiyama T, Kouzuma S, Imakubo T. Identification of optimal operating point of PV modules using neural network for real time maximum power tracking control. IEEE Trans Energy Conversion 1995;10(2):360–7.
- [9] Torres AM, Antunes FLM. An artificial neural network-based real time maximum power tracking controller for connecting a PV system to the grid. Proc IEEE Annu Conf Ind Electron Soc 1998;1:554–8.
- [10] Al-Amoudi A, Zhang L. Application of radial basis function networks for solar-array modelling and maximum power-point prediction. IEEE Proc—Generation Transmission Distribution 2000;147(5):310–6.
- [11] Won CY, Kim DH, Kim SC, Kim WS, Kim HS. A new maximum power point tracker of photovoltaic arrays using fuzzy controller. Proc Annu IEEE Power Electron Specialists Conf 1994;396–403.
- [12] Senjyu T, Uezato K. Maximum power point tracker using fuzzy control for photovoltaic arrays. Proc IEEE Int Conf Ind Technol 1994;143–7.
- [13] Simoes MG, Franceschetti NN. Fuzzy optimisation based control of a solar array system. IEEE Proc Electric Power Appl 1999;146(5):552–8.
- [14] Mahmoud AMA, Mashaly HM, Kandil SA, El Khashab H, Nashed MNF. Fuzzy logic implementation for photovoltaic maximum power tracking. Fuzzy logic implementation for photovoltaic maximum power tracking. Proc 9th IEEE Int Workshop Robot Human Interactive Commun 2000;155–60.
- [15] Zheng L. A practical guide to tune of proportional and integral (PI) like fuzzy controller. IEEE Int Conf Fuzzy Syst 1992;633–40.
- [16] Premrudeepreechacharn S, Poapornsawan T. Fuzzy logic control of predictive current control for grid-connected single phase inverter. Proc 28th IEEE Photovoltaic Specialist Conf 2000;1715–8.